JACS
JOURNAL OF THE AMERICAN CHEMICAL SOCIETY
Article
pubs.acs.org/JACS

Dibenzoheptazethrene Isomers with Different Biradical Characters: An Exercise of Clar's Aromatic Sextet Rule in Singlet Biradicaloids

Zhe Sun,[†] Sangsu Lee,[‡] Kyu Hyung Park,[‡] Xiaojian Zhu,[§] Wenhua Zhang,[∥] Bin Zheng,[⊥] Pan Hu,[†] Zebing Zeng,[†] Soumyajit Das,[†] Yuan Li,[†] Chunyan Chi,[†] Run-Wei Li,[§] Kuo-Wei Huang,*[,⊥] Jun Ding,*[,#] Dongho Kim,*[,‡] and Jishan Wu*[,†,∥]

[†]Department of Chemistry, National University of Singapore, 3 Science Drive 3, 117543 Singapore

[‡]Department of Chemistry, Yonsei University, Seoul 120-749, Korea

[§]Key Laboratory of Magnetic Materials and Devices, Ningbo Institute of Materials Technology and Engineering, Chinese Academy of Sciences, Ningbo 315201, China

[∥]Institute of Materials Research and Engineering, A*STAR, 3 Research Link, 117602 Singapore

[⊥]Division of Physical Science and Engineering and KAUST Catalysis Center, King Abdullah University of Science and Technology (KAUST), Thuwal 23955-6900, Kingdom of Saudi Arabia

[#]Department of Materials Science & Engineering, National University of Singapore, 119260 Singapore

Supporting Information

ABSTRACT: *Clar's aromatic sextet rule* has been widely used for the prediction of the reactivity and stability of polycyclic aromatic hydrocarbons with a *closed-shell* electronic configuration. Recent advances in *open-shell* biradicaloids have shown that the number of aromatic sextet rings plays an important role in determination of their ground states. In order to test the validity of this rule in singlet biradicaloids, the two soluble and stable dibenzoheptazethrene isomers **DBHZ1** and **DBHZ2** were prepared by different synthetic approaches and isolated in crystalline form. These two molecules have different numbers of aromatic sextet rings in their respective biradical resonance forms and thus are expected to exhibit varied singlet biradical character. This assumption was verified by different experimental methods, including nuclear magnetic resonance (NMR), electron spin resonance (ESR), superconducting quantum interference device (SQUID), steady-state and transient absorption spectroscopy (TA), and X-ray crystallographic analysis, assisted by unrestricted symmetry-broken density functional theory (DFT) calculations. **DBHZ2**, with more aromatic sextet rings in the biradical form, was demonstrated to possess greater biradical character than **DBHZ1**; as a result, **DBHZ2** exhibited an intense one-photon absorption (OPA) in the near-infrared region (λ_{abs}^{max} = 804 nm) and a large two-photon absorption (TPA) cross-section ($\sigma^{(2)}_{max}$ = 2800 GM at 1600 nm). This investigation together with previous studies indicates that Clar's aromatic sextet rule can be further extended to the singlet biradicaloids to predict their ground states and singlet biradical characters.

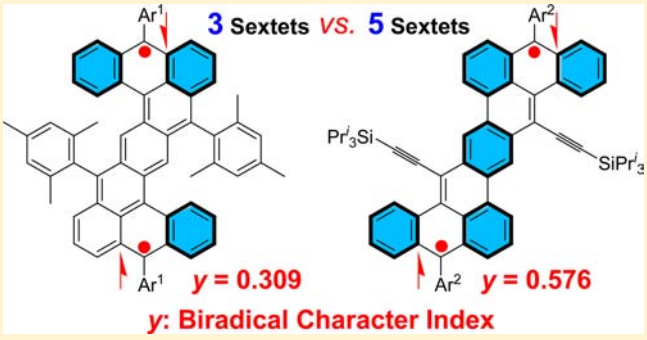

I. INTRODUCTION

The study of open-shell polycyclic hydrocarbons (PHs) with ground state singlet biradical (SB) character is of fundamental importance in understanding the nature of chemical bonding and many chemical/physical phenomena in π-conjugated systems.[1] In addition, their unique optical, electronic, and magnetic properties make them promising candidates for organic electronics,[2] nonlinear optics,[3] spintronics,[4] and energy storage devices.[5] A major challenge in the synthesis and isolation of open-shell PHs is their intrinsic instability, which can be partially overcome by introducing bulky or electron-withdrawing substituents at strategic positions. So far, several types of stable open-shell PHs have been reported, including bisphenalenyls,[6] indenofluorenes,[7] anthenes,[8] extended *p*-quinodimethanes,[9] and zethrenes,[10] which allow a glimpse of their peculiar properties arising from singlet biradical character.

Benzenoid PHs usually can be drawn as two types of resonance structures, a closed-shell Kekulé form and an open-shell biradical form. A straightforward evaluation of the contribution of the biradical resonance form to the ground state is the biradical character y ($0 < y < 1$, 0 representing closed-shell state and 1 representing pure diradical state), which can be obtained either by theoretical calculation on the basis of the natural orbital occupation number (NOON)[11] of the LUMO or by experimental measurements.[12,10c] It was also

Received: October 7, 2013
Published: November 9, 2013

dx.doi.org/10.1021/ja410279j | J. Am. Chem. Soc. 2013, 135, 18229−18236

demonstrated that the physical properties of open-shell singlet biradicaloids are closely related to their biradical characters. Therefore, it is of importance to understand the fundamental structure−biradical character relationship.

Clar's aromatic sextet rule is known as a classic rule to evaluate the stability and reactivity of closed-shell polycyclic aromatic hydrocarbons (PAHs): that is to say, *for benzenoid PAHs with the same chemical composition, the molecule with more aromatic sextet rings shows higher stability and lower reactivity.*[13] This is because the benzene ring containing six π electrons exhibits a large resonance energy, and thus a PAH with more aromatic sextet rings will show higher stability. For example, triphenylene ($C_{18}H_{12}$) is more stable than tetracene ($C_{18}H_{12}$) because two more aromatic sextet rings can be drawn for the former (Figure 1a). Recent studies by Kubo et al.[8,14] disclosed

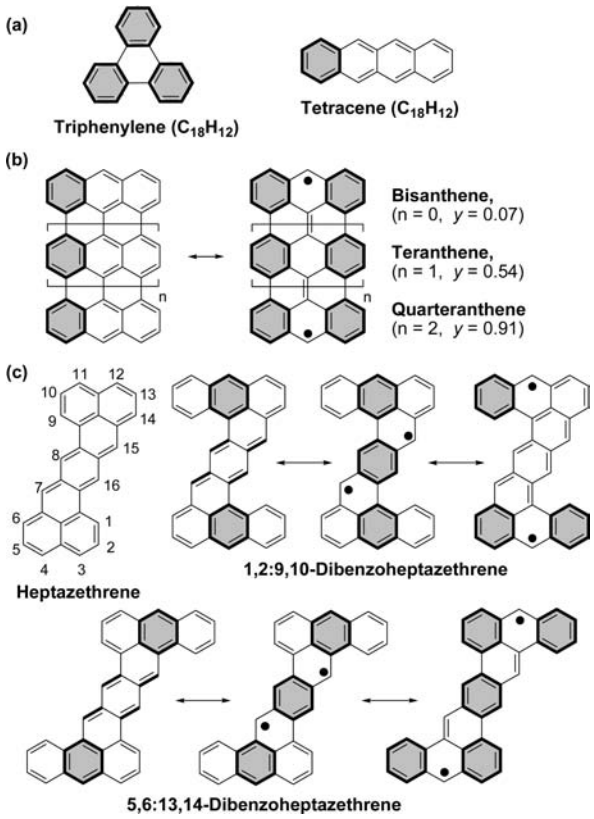

Figure 1. (a) Chemical structures of triphenylene and tetracene. (b) Resonance structures of anthenes. (c) Chemical structure of heptazethrene and the resonance structures of two DBHZ isomers. The benzene rings with bold lines and gray color denote Clar's aromatic sextet rings.

the importance of aromatic stabilization for the ground state of the anthene series: that is, the singlet biradical character y increases from 0.07 to 0.91 from bisanthene to quarteranthene as more aromatic sextet rings form in the biradical species (Figure 1b).[8] Our recent studies on a homologous series of zethrenes also highlighted the importance of additional aromatic sextet rings on stabilizing the biradical structure.[10] In order to examine the validity of Clar's aromatic sextet rule in the open-shell singlet biradical PH systems, a better insight can be provided by systems with the same chemical composition. In this regard, homologous anthenes and zethrenes are not suitable, considering other variables such as conjugation length. However, two dibenzoheptazethrene (DBHZ) isomers (Figure 1c) can be good test beds for our investigations. Heptazethrene (HZ) was theoretically predicted to be a ground-state singlet biradical,[15] but our recent studies showed that the ground state of HZ derivatives was dependent on the substituents and HOMO−LUMO gap.[10] Lateral fusion of two benzenoid rings to the HZ core in different modes can lead to two isomeric structures, 1,2:9,10-dibenzoheptazethrene (isomer 1) and 5,6:13,14-dibenzoheptazethrene (isomer 2) (Figure 1c). For isomer 1, there are two aromatic sextets in the closed-shell quinoidal form and a maximum of three in the biradical form, regardless of the positions of the radicals. However, for isomer 2, two aromatic sextets are present in the quinoidal form while three can be depicted when the two radicals are resident at the bay region and a maximum of five can be drawn when the two radicals are located at the terminal anthracene units. Since the two isomers have the same carbon/hydrogen composition, the discussion of the biradical character can be concentrated on the numbers of Clar aromatic sextet rings. We anticipate that more aromatic sextets for isomer 2 will help to stabilize the biradical resonance form and thus it is expected to show greater biradical character than isomer 1.

On the basis of the resonance structures shown in Figure 1c and our previous investigations on zethrene-based molecules,[10] a reasonable assumption is that the most reactive sites locate at bay regions and terminal zigzag edges. In order to obtain stable and soluble materials, our design is to block the reactive sites with aryl (such as mesityl, *tert*-butylphenyl) or bulky alkyne groups (triisopropylsilylethynyl group). In this work, the two stable dibenzoheptazethrene derivatives **DBHZ1** and **DBHZ2** (Scheme 1) were synthesized and their biradical characters were systematically investigated by various spectroscopic measurements, X-ray crystallographic analysis, and DFT calculations. Our studies provide a proof of concept on how Clar's aromatic sextet rule can be applied to the singlet biradicaloid systems.

II. RESULTS AND DISCUSSION

Synthesis. Two facile synthetic approaches were developed to construct these molecules utilizing either an intramolecular Friedel−Crafts alkylation reaction or an intramolecular Heck coupling reaction as a key step (Scheme 1). For the synthesis of **DBHZ1**, we started from anthracene derivative **1** with the *tert*-butylphenyl group to ensure sufficient solubility for intermediates and the final product. Suzuki coupling of **1** with 1,4-dimethyl-2,5-bis(4,4,5,5-tetramethyl[1.3.2]dioxaborolan-2-yl)-phenyl gave intermediate **2**, the dimethyl groups of which were then transformed into dialdehyde to afford **6** via a bromination−esterification−hydrolysis−oxidation sequence. Then, **6** was treated with mesitylmagnesium bromide to give diol **7**, which was subjected to a Friedel−Crafts alkylation reaction promoted by $BF_3{\cdot}OEt_2$ to afford compound **8**.[16] **DBHZ1** was obtained as a blue solid by oxidation of **8** with DDQ. On the other hand, **DBHZ2** was prepared starting from anthracene derivative **9** with mesityl substitution.[17] The as-formed lithium reagent of **9** reacted with 2,5-dibromobenzene-1,4-dicarbaldehyde to afford the diol **10**, which then underwent Swern oxidation[18] to yield **11**. Subsequently, the intramolecular Heck reaction[19] of **11** catalyzed by $Pd(OAc)_2$ gave the diketone precursor **12**, which was treated with triisopropylsilyl ethynylene lithium reagent followed by reduction with $SnCl_2$ to give **DBHZ2** as a green solid. The structures of **DBHZ1** and **DBHZ2** have been identified unambiguously by 1D $^1H/^{13}C$ NMR and 2D COSY NMR spectroscopy, high-resolution mass

dx.doi.org/10.1021/ja410279j | J. Am. Chem. Soc. 2013, 135, 18229−18236

Scheme 1. Synthesis of DBHZ1 and DBHZ2[a]

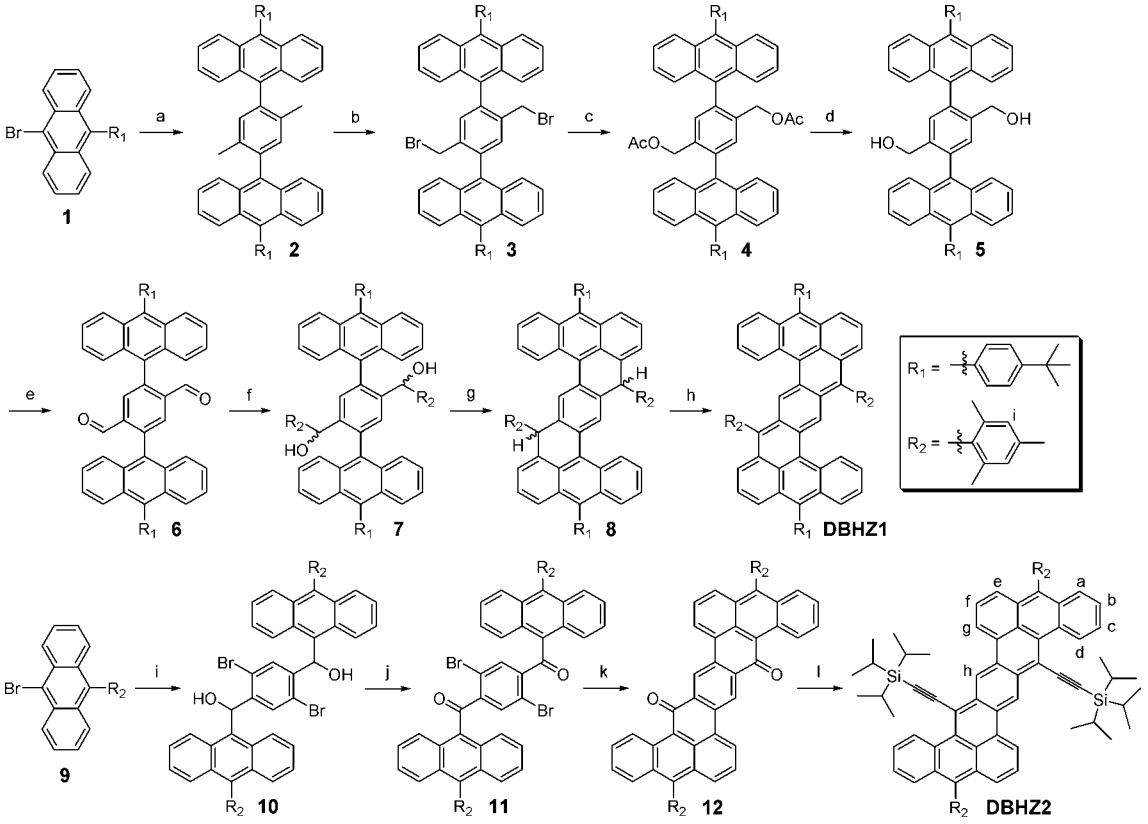

[a]Reagents and conditions: (a) 1,4-dimethyl-2,5-bis(4,4,5,5-tetramethyl[1,3,2]dioxaborolan-2-yl)phenyl, $Pd_2(dba)_3$, DPEPhos, K_2CO_3 (aq), toluene/ethanol, reflux, 43%; (b) NBS, BPO, CCl_4, reflux; (c) KOAc, Bu_4NBr, DMF, 100 °C, 57% in two steps from **2**; (d) KOH (aq), THF/ethanol, reflux; (e) PCC, DCM, room temperature, 50% in two steps from **4**; (f) mesitylmagnesium bromide, THF, room temperature; (g) $BF_3{\cdot}OEt_2$, CH_2Cl_2, room temperature; (h) DDQ, toluene, room temperature, 45% in three steps from **6**; (i) (1) *n*-BuLi, THF, −78 °C, (2) 2,5-dibromobenzene-1,4-dicarbaldehyde, THF, −78 °C to room temperature, 35%; (j) $(CF_3CO_2)O$/DMSO, CH_2Cl_2, −78 °C, 76%; (k) $Pd(OAc)_2$, KOAc, TBAB, DMAc, 160 °C, 27%; (l) (i) $LiCCSi(i\text{-}Pr)_3$, THF; (ii) $SnCl_2$, 75%. Abbreviations: NBS, *N*-bromosuccinimide; BPO, benzoyl peroxide; PCC, pyridinium chlorochromate; DDQ, 2,3-dichloro-5,6-dicyano-1,4-benzoquinone; TBAB, tetrabutylammonium bromide.

spectrometry (see the Supporting Information), and crystallographic analysis (vide infra).

Magnetic Properties. **DBHZ1** showed well-resolved sharp peaks in the ^{1}H NMR spectrum in C_6D_6 solution at room temperature, and it is ESR silent. In contrast, no NMR signals in the aromatic region were observed for **DBHZ2** at room temperature and a progressive sharpening of peaks was found when the temperature was lowered in THF-d_8 solution (Figure 2). The NMR peaks can be assigned to the structure of **DBHZ2** with the help of 2D-COSY NMR spectroscopy (Figure S1 in the Supporting Information). This behavior is common for many other singlet biradical PHs,[8,10] which can be explained by the presence of thermally excited triplet species caused by the small singlet−triplet energy gap $\Delta E_{SB\text{-}TB}$. A broad ESR signal with g tensor of g_e = 2.0027 was observed from a toluene solution of **DBHZ2** (Figure 3a), and the signal intensity decreased with a decrease in temperature, indicating a singlet biradical ground state for **DBHZ2**. The temperature-dependent magnetic susceptibility behavior of **DBHZ2** (5−380 K) obtained by SQUID measurements revealed that it indeed has a singlet biradical ground state (Figure 3b). An exchange interaction energy ($2J/k_B$, i.e., $\Delta E_{SB\text{-}TB}$) of −1859.6 K (−3.7 kcal/mol) was estimated by a careful fitting of the data using the Bleaney−Bowers equation:[20]

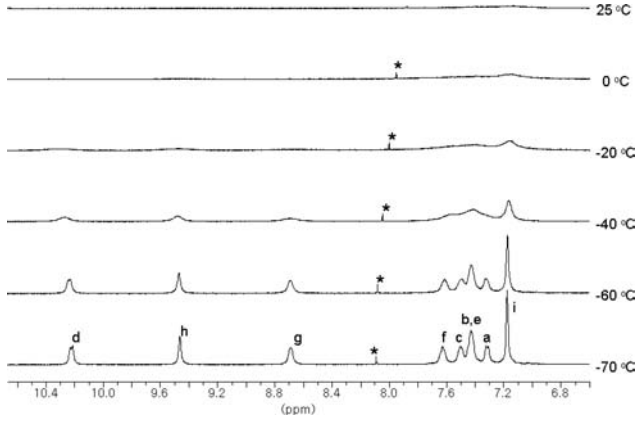

Figure 2. Variable-temperature ^{1}H NMR spectra (aromatic region) of **DBHZ2** in THF-d_8 and assignments of aromatic protons. Assignments refer to the structure shown in Scheme 1. The peak labeled with an asterisk is from the impurity in THF-d_8.

$$\chi = \frac{N\beta^2 g^2}{3kT}\left[1 + \frac{1}{3}\exp\left(\frac{J_{s-t}}{kT}\right)\right]^{-1}$$

where χ is the magnetic susceptibility, N is Avogadro's number, β is the Bohr magneton, g is the magnetic field splitting factor, k

dx.doi.org/10.1021/ja410279j | J. Am. Chem. Soc. 2013, 135, 18229−18236

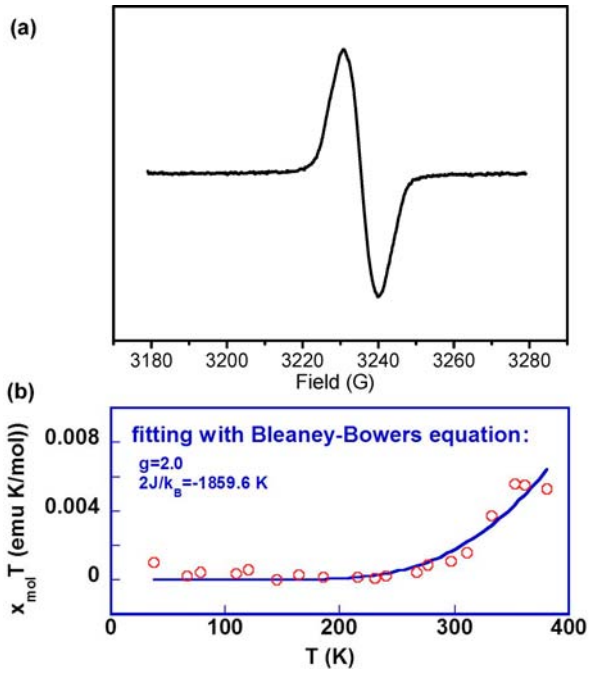

Figure 3. (a) ESR spectrum of **DBHZ2** in toluene solution measured at room temperature. (b) $\chi T-T$ plot for the solid **DBHZ2**. The measured data were plotted as open circles, and the fitting curve was drawn using the Bleaney−Bowers equation with g = 2.00.

is Boltzmann's constant, T is the temperature, and J is the exchange integral. This small value again explains the presence of an ESR signal in toluene solution and the line broadening of the NMR at room temperature for **DBHZ2**.

X-ray Crystallographic Analysis. Single crystals suitable for X-ray crystallographic analysis were obtained for both **DBHZ1** and **DBHZ2** by slow diffusion of methanol into a chloroform solution, and the structures are shown in Figure 4.[21] For both molecules, the DBHZ core slightly deviates from planarity due to steric congestion at the cove region (**DHBZ1**) or between the C≡C bond and the anthracene unit (**DBHZ2**), with a torsional angles of 33.9 and 17.6°, respectively (Figure 4a,b). For **DBHZ1**, there is obviously a bond length alternation in the central *p*-quinodimethane subunit, indicating that the quinoidal resonance form has a significant contribution to the ground state electronic structure (Figure 4c). However, the bond *a* (1.429 Å) is much shorter than a typical C(sp^2)−C(sp^2) bond (~1.47 Å) and the bond *b* (1.376 Å) is much longer than the double bond in olefins (1.33−1.34 Å), which means the quinoidal character is diminished by the emergence of the biradical contribution. Therefore, **DBHZ1** is better described as a borderline molecule with a ground state between a closed-shell quinoid and a singlet biradical, which is in accordance with the observed ESR silence. For **DBHZ2**, the central benzene ring is almost aromatic, as shown from the uniform bond lengths (1.399, 1.409, 1.411 Å). The bonds *c* (1.457 Å) and *d* (1.454 Å) are more like single bonds, presumably due to the large contribution of the second resonance form (Figure 1c) to the ground state and steric hindrance induced bond length elongation. The calculated nucleus independent chemical shift (NICS(1)zz)[22] values of **DBHZ1** showed less aromatic character for the central benzene ring (−11.6 ppm) (Figure 4c), indicating a large contribution from the quinoidal structure. In contrast, the NICS(1)zz values of **DBHZ2** displayed greater aromatic benzenoid character for the central

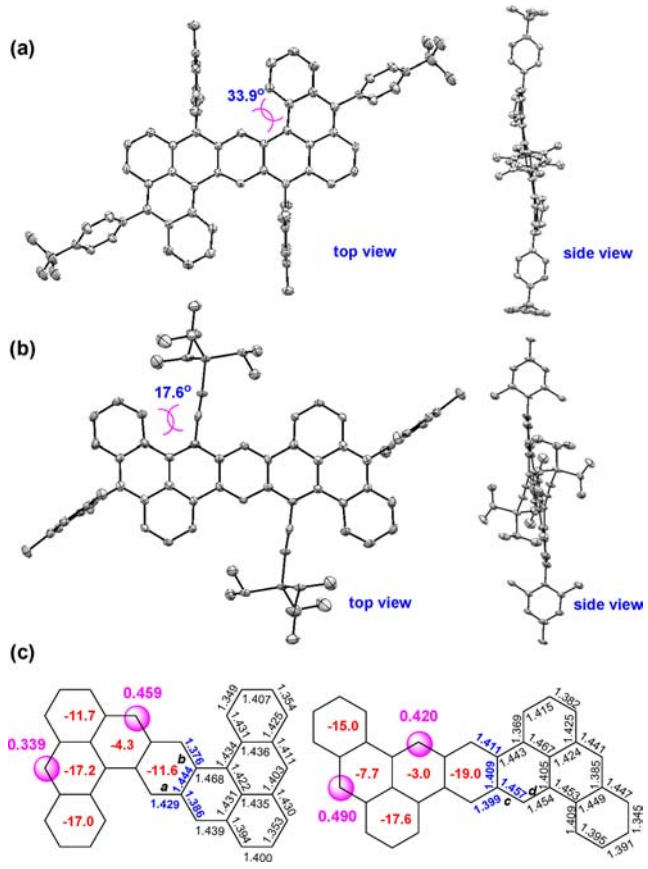

Figure 4. ORTEP drawings of (a) **DBHZ1** and (b) **DBHZ2** measured at 123 K. The hydrogen atoms are omitted for clarity. (c) Mean values of bond lengths (Å) and calculated NICS(1)zz values in the DBHZ core for **DBHZ1** and **DBHZ2**. The numbers given in pink denote the spin densities of the specific carbon atoms.

benzene ring (−19.0 ppm) and two terminal rings in the anthracene unit (−15.0 and −17.6 ppm), implying a significant contribution from the third resonance form (Figure 1c, the form with five sextet rings). The calculated spin densities at the specific carbon atoms (Figure 4c) also indicate that the third resonance form contributes the most to the ground state of **DBHZ2**. For **DBHZ1**, however, the second resonance contributes more than the third resonance.

DFT Calculations. DFT calculations (UCAM-B3LYP/6-31G(d,p)) were conducted to understand the ground states of both molecules. It was found that the energy of the SB state is 6.9 and 7.6 kcal/mol lower than the triplet biradical (TB) and closed-shell (CS) states for **DBHZ1**, respectively, and the energy of the SB state is 3.3 and 13.4 kcal/mol lower than those of the TB and CS states for **DBHZ2**, respectively. Therefore, both molecules feature a singlet biradical ground state. The calculated singlet−triplet gap of **DBHZ2** is in line with that determined by SQUID measurements (−3.7 kcal/mol), which further explains the observed NMR line broadening and ESR signal. On the other hand, the relatively larger singlet−triplet gap of **DBHZ1** (−6.9 kcal/mol) agrees well with the sharp NMR peaks and ESR silence. On the basis of the UCAM-B3LYP method, the biradical characters *y* for **DBHZ1** and **DBHZ2** were calculated as 0.309 and 0.576, respectively, which are in agreement with magnetic measurements and X-ray analysis. The molecular orbital profiles exhibit a typical disjointed character for the ground-state singlet biradicals

dx.doi.org/10.1021/ja410279j | J. Am. Chem. Soc. 2013, 135, 18229−18236

(Figure 5a,b) and the spin densities are evenly delocalized over the whole π-conjugated framework for both molecules (Figure 5c), which are similar to other higher order zethrene biradicals such as heptazethrene dimide and octazethrene.[10] All of the calculation results clearly point out a larger biradical character for **DBHZ2** than for **DBHZ1**, consistent with our anticipation from numbers of Clar aromatic sextet rings in the biradical resonance forms.

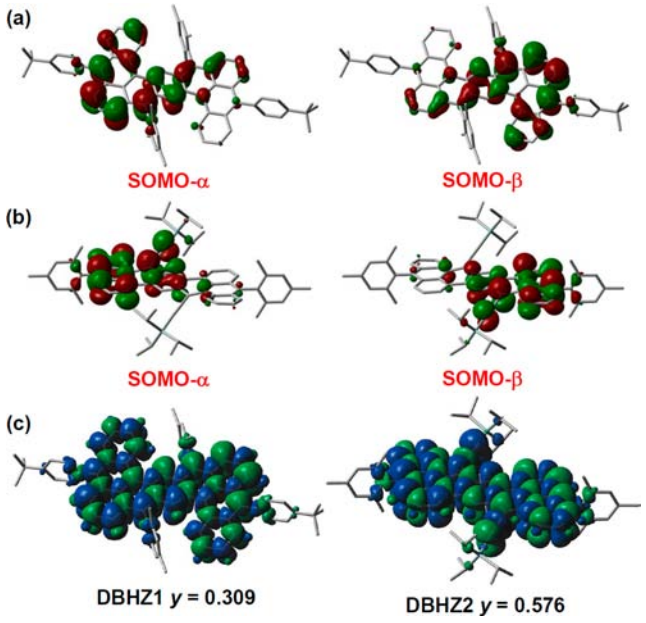

Figure 5. Calculated (UCAM-B3LYP) SOMOs of α and β electrons of (a) **DBHZ1** and (b) **DBHZ2**. (c) Calculated spin density distributions of **DBHZ1** and **DBHZ2**. The blue and green surfaces represent α and β spin densities, respectively.

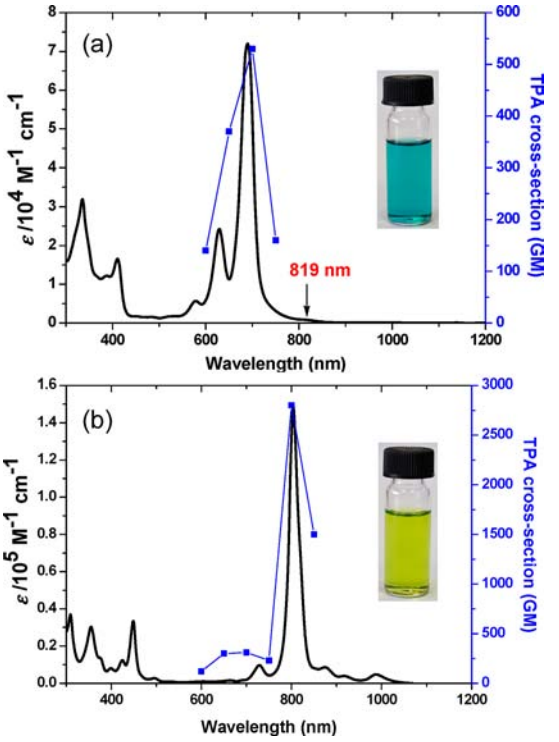

Figure 6. OPA spectra (solid line and left vertical axis) and TPA spectra (blue symbols and right vertical axis) of (a) **DBHZ1** and (b) **DBHZ2**. TPA spectra are plotted at $\lambda_{ex}/2$. Insets give photographs of the solutions in chloroform.

Optical Properties. **DBHZ1** is blue in chloroform solution, and its absorption spectrum shows a p band with a maximum peak at 687 nm ($\varepsilon = 7.2 \times 10^4$ M^{-1} cm^{-1}) and a shoulder peak at 628 nm, which is common for many closed-shell PHs such as rylenes and acenes (Figure 6a and Table 1).[23] However, a weak absorption tail can be also observed at longer wavelengths up to 850 nm, which is usually related to the open-shell singlet biradicals.[8,10] This phenomenon again supports the borderline character of **DBHZ1** between a quinoidal structure and a biradical structure, as revealed by X-ray analysis and calculations. In sharp contrast, the lime-colored solution of **DBHZ2** in chloroform displays a typical absorption feature for singlet biradicaloid molecules with an intense absorption at 804 nm ($\varepsilon = 1.5 \times 10^5$ M^{-1} cm^{-1}) and several small bands in the lower energy region (Figure 6b). The weak absorption bands in the low-energy region likely originate from admixing the doubly excited electronic configuration (H,H → L,L) into the ground state.[24] No fluorescence is observed for both compounds, which is a common behavior of biradicaloids. Despite the large π conjugation and the biradical character, both **DBHZ1** and **DBHZ2** exhibit a good photostability with a half-life time ($t_{1/2}$) of more than 1 week in solution upon exposure to ambient air and light conditions (Figures S2−S7 in the Supporting Information), which can be explained by the proper blocking of the most reactive sites and the large spin delocalization shown in the spin density map. It is also worth noting that the intense and sharp near-IR absorption and weak absorption at visible region for **DBHZ2** make it almost transparent at lower concentrations in solution, which meets the criteria for many technological applications for near-IR dyes.

The excited-state dynamics of both isomers were probed by femtosecond transient absorption (TA) measurements (Figure 7 and Figure S8 in the Supporting Information). The TA spectrum of **DBHZ1** exhibited a ground-state bleaching (GSB) signal around 680 nm together with weak excited-state absorption (ESA) bands in the 450−600 and 720−800 nm spectral regions. For **DBHZ2**, a GSB signal was observed around 800 nm and an intense ESA band appeared in the 450−750 nm spectral region. The singlet excited-state lifetimes of **DBHZ1** and **DBHZ2** were estimated to be 670 and 330 ps, respectively, and the short singlet excited-state lifetimes explain the nonfluorescent behavior well. In comparison to **DBHZ1**, the smaller singlet excited-state lifetime of **DBHZ2** could be correlated to a faster nonradiative internal conversion process arising from a smaller energy gap between the lowest excited state and the singlet biradical ground state.

Recent theoretical and experimental studies have indicated that a moderate biradical character could enhance TPA activity for PH systems.[3,9,15] Therefore, two-photon absorption measurements for **DBHZ1** and **DBHZ2** were conducted by the Z-scan technique in toluene in the near-IR region from 1200 to 1700 nm, where one-photon absorption contribution is negligible (Figure 6 and Figure S9 in the Supporting Information). **DBHZ1** exhibited the cross-section $\sigma^{(2)}_{max}$ = 530 GM at 1400 nm, which is much smaller than for **DBHZ2** ($\sigma^{(2)}_{max}$ = 2800 GM at 1600 nm). Such differences in nonlinear optical properties must be related to the greater biradical character of the latter. Notably, in comparison to the TPA cross-sections of a heptazethrene derivative (**HZ-DI**; 920 GM

dx.doi.org/10.1021/ja410279j | J. Am. Chem. Soc. 2013, 135, 18229−18236

Table 1. Photophysical and electrochemical data of DBHZ1 and DBHZ2[a]

	λ_{abs} (nm)	ε_{max} (M^{-1} cm^{-1})	τ (ps)	$\sigma^{(2)}{}_{max}$ (GM)	$E_{1/2}{}^{ox}$ (V)	$E_{1/2}{}^{red}$ (V)	HOMO (eV)	LUMO (eV)	$E_g{}^{EC}$ (eV)	$E_g{}^{opt}$ (eV)
DBHZ1	819, 687, 628	72000	670	530 (1400 nm)	−0.20	−1.72	−4.54	−3.20	1.34	1.46
					0.26	−2.04				
DBHZ2	989, 919	148900	330	2800 (1600 nm)	−0.18	−1.34	−4.57	−3.55	1.02	1.20
	879, 804, 727				0.19	−1.68				

[a]Definitions: λ_{abs}, absorption maxima measured in $CHCl_3$; ε_{max}, molar extinction coefficient measured at absorption maximum; τ, the singlet excited-state lifetime obtained from TA; $\sigma^{(2)}{}_{max}$, the maximum TPA cross section. $E_{1/2}{}^{ox}$ and $E_{1/2}{}^{red}$ are the half-wave potentials for respective oxidation and reduction waves with Fc/Fc^+ as reference. HOMO and LUMO energy levels were calculated according to the equations HOMO = $-(4.8 + E_{ox}{}^{onset})$ and LUMO = $-(4.8 + E_{red}{}^{onset})$, where $E_{ox}{}^{onset}$ and $E_{red}{}^{onset}$ are the onset potentials of the first oxidative and reductive redox wave, respectively. $E_g{}^{EC}$ is the electrochemical energy gap derived from LUMO−HOMO, and $E_g{}^{opt}$ is the optical energy gap derived from the lowest energy absorption onset in the absorption spectra.

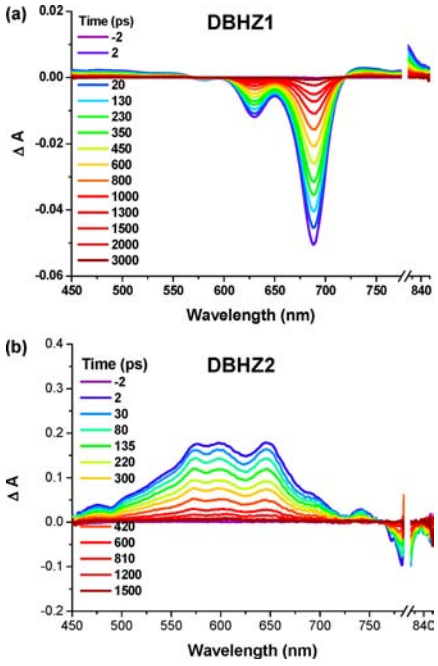

Figure 7. Transient absorption spectra of (a) **DBHZ1** and (b) **DBHZ2** recorded in toluene.

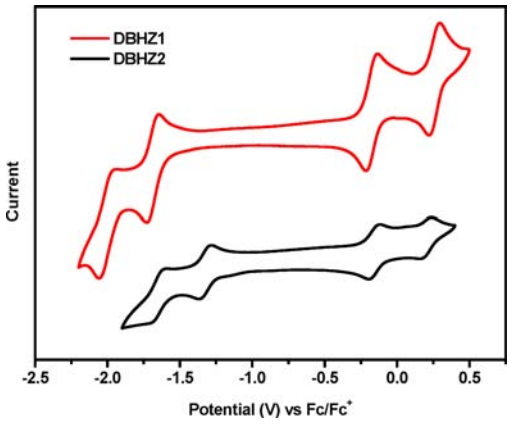

Figure 8. Cyclic voltammograms of **DBHZ1** and **DBHZ2** in CH_2Cl_2 with 0.1 M Bu_4NPF_6 as supporting electrolyte, Ag/AgCl as the reference electrode, Au disk as the working electrode, Pt wire as the counter electrode, and the scan rate at 50 mV/s.

at 1250 nm, y = 0.159) and an octazethrene derivative (**OZ-TIPS**; 1200 GM at 1250 nm, y = 0.56),[10c] **DBHZ2** also exhibited a large enhancement. Therefore, a TPA cross-section−singlet biradical character relationship can be established for zethrene-based compounds.

Electrochemical Properties. Cyclic voltammertry (CV, Figure 8) and differential pulse voltammetry (DPV) (Figure S10 in the Supporting Information) were employed to investigate the electrochemical properties of **DBHZ1** and **DBHZ2**, and both compounds display well-resolved four-stage amphoteric redox behavior. **DBHZ1** gave two oxidation waves at $E_{1/2}{}^{ox}$ = −0.20, 0.26 V and two reduction waves at $E_{1/2}{}^{red}$ = −1.72, −2.04 V, while **DBHZ2** showed two oxidation waves at $E_{1/2}{}^{ox}$ = −0.18, 0.19 V and two reduction waves at $E_{1/2}{}^{red}$ = −1.34, −1.68 V (vs Fc/Fc^+, Fc = ferrocene). The electrochemical energy gaps were determined as 1.34 and 1.02 eV for **DBHZ1** and **DBHZ2**, respectively, from the onset potentials of the first oxidation and reduction wave, which are consistent with those obtained from the optical onset (Table 1). Such low-energy gaps are believed to be a crucial prerequisite for the formation of a singlet biradical ground state.

The multistage reversible redox waves and the large separation between the redox waves allow us to attain the singly and doubly charged species by a chemical approach. Indeed, the stable radical cations and dications of **DBHZ1** and **DBHZ2** were prepared by a stepwise oxidative titration with $SbCl_5$ in CH_2Cl_2 at room temperature and the obtained UV−vis−near-IR absorption spectra for the cationic species are shown in Figure 9a,c. In the course of chemical oxidation, sequential oxidation to the radical cation and then the dication were observed when 9 and 20 equiv of $SbCl_5$ were added for **DBHZ1** and when 5 and 11 equiv of $SbCl_5$ were added for **DBHZ2** (Figure S11 in the Supporting Information). Moreover, both of the obtained dications can be reduced to the neutral states by Zn powder, in accordance with the reversible oxidative waves observed in CV measurements (Figure S11 in the Supporting Information). Notably, all the cationic species exhibited reasonable stability in solution, which allowed further investigation into their physical properties. As shown in Figure 9b,d, ESR spectra were recorded for the radical cation species of **DBHZ1** and **DBHZ2** in CH_2Cl_2 solution at room temperature, and the radical cation of **DBHZ1** exhibited an observable fine structure with g_e = 2.0026, while the radical cation of **DBHZ2** showed a single-line signal with g_e = 2.0027. No ESR signals were observed for the dications. The good stability of the radical cations and dications for both DBHZ isomers can be explained by the recovery of aromaticity of the central benzenoid ring in both cases (Figure 9e).

III. CONCLUSION

In summary, the two soluble and stable DBHZ isomers **DBHZ1** and **DBHZ2** were prepared by two different synthetic strategies. The substitutions of bulky aryl and alkyne groups

dx.doi.org/10.1021/ja410279j | J. Am. Chem. Soc. 2013, 135, 18229−18236

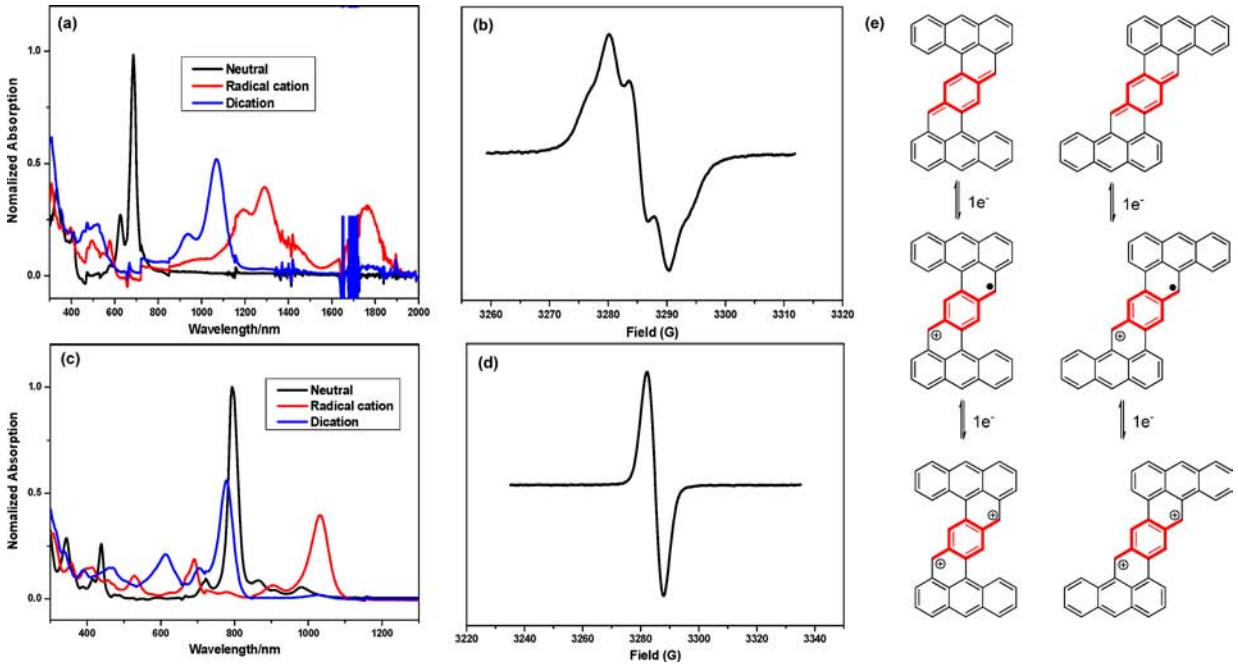

Figure 9. Absorption spectra of neutral compounds, radical cations, and dications of (a) **DBHZ1** and (c) **DBHZ2** recorded in CH_2Cl_2. ESR spectra of (b) **DBHZ1** radical cation (g_e = 2.0026) and (d) **DBHZ2** radical cation (g_e = 2.0027) in CH_2Cl_2 (10^{-3} M) solution at 298 K. (e) Schematic representation of the one-electron-oxidation process in DBHZ isomers.

guarantee the stability and crystallinity, which facilitated the investigation. Their electronic structures in the ground state were systematically studied by various experimental methods and DFT calculations, and the results clearly demonstrated a much greater biradical character of **DBHZ2** in comparison to **DBHZ1**. This difference in biradical character between two isomeric structures can be explained by the different numbers of aromatic sextet rings in the biradical resonance forms. With this study, Clar's aromatic sextet rule can be extended from closed-shell benzenoid PAHs to open-shell singlet biradicaloids (at least applicable to our systems): that is to say, *for benzenoid polycyclic hydrocarbons with the same chemical composition, the molecule with more aromatic sextet rings in the biradical resonance form exhibits greater singlet biradical character*. We believe that our findings provide useful guidance for the design and study of PHs with open-shell singlet biradical ground states in the future.

From another perspective, the obtained DBHZ derivatives exhibited interesting physical properties associated with the biradical character. For example, **DBHZ2** showed intense OPA absorption in the near-IR region and a large TPA cross-section, and stable cationic species for both **DBHZ1** and **DBHZ2** were chemically accessible due to their pro-aromatic nature. Together with their good stability, the DBHZ derivatives reported in this study represent promising candidates in materials science.

■ ASSOCIATED CONTENT

Supporting Information

Synthetic procedures and characterization data for all new compounds, general experimental methods, additional spectroscopic data, DFT calculation details, and crystallographic data. This material is available free of charge via the Internet at http://pubs.acs.org.

■ AUTHOR INFORMATION

Corresponding Author

chmwuj@nus.edu.sg; dongho@yonsei.ac.kr; msedingj@nus.edu.sg; kuowei.huang@kaust.edu.sa

Notes

The authors declare no competing financial interest.

■ ACKNOWLEDGMENTS

J.W. acknowledges financial support from a MOE Tier 2 grant (MOE2011-T2-2-130) and IMRE Core funding (IMRE/13-1C0205). The work at Yonsei University was supported by the Midcareer Researcher Program (2010-0029668) and the Global Research Laboratory (2013K1A1A2A02050183) through the National Research Foundation of Korea (NRF) funded by the Ministry of Science, ICT (Information and Communication Technologies) and Future Planning. K.-W.H. acknowledges financial support from KAUST.

■ REFERENCES

(1) (a) Lambert, C. *Angew. Chem., Int. Ed.* **2011**, *50*, 1756−1758. (b) Morita, Y.; Suzuki, K.; Sato, S.; Takui, T. *Nat. Chem.* **2011**, *3*, 197−204. (c) Sun, Z.; Wu, J. *J. Mater. Chem.* **2012**, *22*, 4151−4160. (d) Sun, Z.; Ye, Q.; Chi, C.; Wu, J. *Chem. Soc. Rev.* **2012**, *41*, 7857−7889. (e) Shimizu, A.; Hirao, Y.; Kubo, T.; Nakano, M.; Botek, E.; Champagne, B. *AIP Conf. Proc.* **2012**, *1504*, 399−405. (f) Sun, Z.; Zeng, Z.; Wu, J. *Chem. Asian J.* **2013**, DOI: 10.1002/asia.201300560. (g) Abe, M. *Chem. Rev.* **2013**, *113*, 7011−7088.

(2) (a) Chikamatsu, M.; Mikami, T.; Chisaka, J.; Yoshida, Y.; Azumi, R.; Yase, K. *Appl. Phys. Lett.* **2007**, *91*, 043506. (b) Chase, D. T.; Fix, A. G.; Kang, S. J.; Rose, B. D.; Weber, C. D.; Zhong, Y.; Zakharov, L. N.; Lonergan, M. C.; Nuckolls, C.; Haley, M. M. *J. Am. Chem. Soc.* **2012**, *134*, 10349−10352. (c) Lee, J.; Jadhav, P.; Reusswig, P. D.; Yost, S. R.; Thompson, N. J.; Congreve, D. N.; Hontz, E.; Van Voorhis, T.; Baldo, M. A. *Acc. Chem. Res.* **2013**, *46*, 1300−1311.

(3) Kamada, K.; Ohta, K.; Kubo, T.; Shimizu, A.; Morita, Y.; Nakasuji, K.; Kishi, R.; Ohta, S.; Furukawa, S. I.; Takahashi, H.; Nakano, M. *Angew. Chem., Int. Ed.* **2007**, *46*, 3544−3546.

(4) Son, Y. W.; Cohen, M. L.; Louie, S. G. *Phys. Rev. Lett.* **2006**, *97*, 216803.
(5) Morita, Y.; Nishida, S.; Murata, T.; Moriguchi, M.; Ueda, A.; Satoh, M.; Arifuku, K.; Sato, K.; Takui, T. *Nat. Mater.* **2011**, *10*, 947−951.
(6) (a) Ohashi, K.; Kubo, T.; Masui, T.; Yamamoto, K.; Nakasuji, K.; Takui, T.; Kai, Y.; Murata, I. *J. Am. Chem. Soc.* **1998**, *120*, 2018−2027. (b) Kubo, T.; Sakamoto, M.; Akabane, M.; Fujiwara, Y.; Yamamoto, K.; Akita, M.; Inoue, K.; Takui, T.; Nakasuji, K. *Angew. Chem., Int. Ed.* **2004**, *43*, 6474−6479. (c) Shimizu, A.; Kubo, T.; Uruichi, M.; Yakushi, K.; Nakano, M.; Shiomi, D.; Sato, K.; Takui, T.; Hirao, Y.; Matsumoto, K.; Kurata, H.; Morita, Y.; Nakasuji, K. *J. Am. Chem. Soc.* **2010**, *132*, 14421−14428. (d) Shimizu, A.; Hirao, Y.; Matsumoto, K.; Kurata, H.; Kubo, T.; Uruichi, M.; Yakushi, K. *Chem. Commun.* **2012**, *48*, 5629−5631.
(7) (a) Chase, D. T.; Rose, B. D.; McClintock, S. P.; Zakharov, L. N.; Haley, M. M. *Angew. Chem., Int. Ed.* **2011**, *50*, 1127−1130. (b) Shimizu, A.; Tobe, Y. *Angew. Chem., Int. Ed.* **2011**, *50*, 6906−6910. (c) Shimizu, A.; Kishi, R.; Nakano, M.; Shiomi, D.; Sato, K.; Takui, T.; Hisaki, I.; Miyata, M.; Tobe, Y. *Angew. Chem., Int. Ed.* **2013**, *52*, 6076−6079.
(8) (a) Konishi, A.; Hirao, Y.; Nakano, M.; Shimizu, A.; Botek, E.; Champagne, B.; AShiomi, D.; Sato, K.; Takui, T.; Matsumoto, K.; Kurata, H.; Kubo, T. *J. Am. Chem. Soc.* **2010**, *132*, 11021−11023. (b) Konishi, A.; Hirao, Y.; Matsumoto, K.; Kurata, H.; Kishi, R.; Shigeta, Y.; Nakano, M.; Tokunaga, K.; Kamada, K.; Kubo, T. *J. Am. Chem. Soc.* **2013**, *135*, 1430−1437.
(9) (a) Zeng, Z.; Sung, Y. M.; Bao, N.; Tan, D.; Lee, R.; Zafra, J. L.; Lee, B. S.; Ishida, M.; Ding, J.; López Navarrete, J. T.; Li, Y.; Zeng, W.; Kim, D.; Huang, K.-W.; Webster, R. D.; Casado, J.; Wu, J. *J. Am. Chem. Soc.* **2012**, *134*, 14513−14525. (b) Zeng, Z.; Ishida, M.; Zafra, J. L.; Zhu, X.; Sung, Y. M.; Bao, N.; Webster, R. D.; Lee, B. S.; Li, R.-W.; Zeng, W.; Li, Y.; Chi, C.; López Navarrete, J. T.; Ding, J.; Casado, J.; Kim, D.; Wu, J. *J. Am. Chem. Soc.* **2013**, *135*, 6363−6371. (c) Zeng, Z.; Lee, S.; Zafra, J. L.; Ishida, M.; Zhu, X.; Sun, Z.; Ni, Y.; Webster, R. D.; Li, R.-W.; López Navarrete, J. T.; Chi, C.; Ding, J.; Casado, J.; Kim, D.; Wu, J. *Angew. Chem., Int. Ed.* **2013**, *52*, 8561−8565.
(10) (a) Sun, Z.; Huang, K.-W.; Wu, J. *Org. Lett.* **2010**, *12*, 4690−4693. (b) Sun, Z.; Huang, K.-W.; Wu, J. *J. Am. Chem. Soc.* **2011**, *133*, 11896−11899. (c) Li, Y.; Heng, W.-K.; Lee, B. S.; Aratani, N.; Zafra, J. L.; Bao, N.; Lee, R.; Sung, Y. M.; Sun, Z.; Huang, K.-W.; Webster, R. D.; López Navarrete, J. T.; Kim, D.; Osuka, A.; Casado, J.; Ding, J.; Wu, J. *J. Am. Chem. Soc.* **2012**, *134*, 14913−14922. (d) Sun, Z.; Wu, J. *J. Org. Chem.* **2013**, *78*, 9032−9040. (e) Zeng, W.; Ishida, M.; Lee, S.; Sung, Y.; Zeng, Z.; Ni, Y.; Chi, C.; Kim, D.-H.; Wu, J. *Chem. Eur. J.* **2013**, DOI: 10.1002/chem.201302023.
(11) Döhnert, D.; Koutecký, J. *J. Am. Chem. Soc.* **1980**, *102*, 1789−1796.
(12) Kamada, K.; Ohta, K.; Shimizu, A.; Kubo, T.; Kishi, R.; Takahashi, H.; Botek, E.; Champagne, B.; Nakano, M. *J. Phys. Chem. Lett.* **2010**, *1*, 937−940.
(13) Clar, E. *The Aromatic Sextet*; Wiley: London, 1972.
(14) Shimizu, A.; Hirao, Y.; Kubo, T.; Nakano, M.; Botek, E.; Champagne, B. *AIP Conf. Proc.* **2012**, *1504*, 399−405.
(15) Nakano, M.; Kishi, R.; Takebe, A.; Nate, M.; Takahashi, H.; Kubo, T.; Kamada, K.; Ohta, K.; Champagne, B.; Botek, E. *Comput. Lett.* **2007**, *3*, 333−338.
(16) Pawlicki, M.; Morisue, M.; Davis, N. K. S.; McLean, D. G.; Haley, J. E.; Beuerman, E.; Drobizhev, M.; Rebane, A.; Thompson, A. L.; Pascu, S. I.; Accorsi, G.; Armaroli, N.; Anderson, H. L. *Chem. Sci.* **2012**, *3*, 1541−1547.
(17) We tried to introduce the same substituents at the similar positions for **DBHZ1** and **DBHZ2**; however, the mesityl group is not tolerant to the bromination reaction in the synthetic sequence to **DBHZ1**, and the TIPS group is not tolerant to the cyclization conditions. Moreover, an attempt to treat diketone **12** with mesitylmagnesium bromide followed by reduction failed to give the corresponding product. Nevertheless, we think the substituents do not have a significant effect on the biradical character discussed in this work.
(18) Pérez-Trujillo, M.; Virgili, A.; Molins, E. *Tetrahedron: Asymmetry* **2004**, *15*, 1615−1621.
(19) (a) Echavarren, A. M.; Gómez-Lor, B.; González, J. J.; Frutosa, Ó. *Synlett* **2003**, *5*, 585−597. (b) Preis, E.; Scherf, U. *Macromol. Rapid Commun.* **2006**, *27*, 1105−1109.
(20) Bleaney, B.; Bowers, K. D. *Proc. R. Soc. London Ser. A* **1952**, *214*, 451−465.
(21) (a) Crystallographic data for **DBHZ1**: $C_{151}H_{131}Cl_9$, M_w = 2264.61; triclinic; space group $P\bar{1}$; a = 15.5797(7) Å, b = 19.5366(9) Å, c = 22.6289(11) Å, α = 71.380(2)°, β = 76.171(2)°, γ = 67.194(2)°; V = 5964.3(5) Å^3; Z = 2; ρ_{calcd} = 1.261 Mg/m^3; R1 = 0.0996, wR2 = 0.2302 ($I > 2\sigma(I)$); R1 = 0.1196, wR2 = 0.2454 (all data). (b) Crystallographic data for **DBHZ2**: $C_{76}H_{80}Si_2$, M_w = 1049.58; triclinic; space group $P\bar{1}$; a = 13.9671(12) Å, b = 14.3263(13) Å, c = 15.9903(15) Å, α = 102.783(7)°, β = 107.815(6)°, γ = 90.531(6)°; V = 2960.5(5) Å^3; Z = 2; ρ_{calcd} = 1.177 Mg/m^3; R1 = 0.1472, wR2 = 0.3233 ($I > 2\sigma(I)$); R1 = 0.2226, wR2 = 0.3807 (all data).
(22) Fallah-Bagher-Shaidaei, H.; Wannere, C. S.; Corminboeuf, C.; Puchta, R.; Schleyer, P. v. R. *Org. Lett.* **2006**, *8*, 863−866.
(23) (a) Weil, T.; Vosch, T.; Hofkens, J.; Peneva, K.; Müllen, K. *Angew. Chem., Int. Ed.* **2010**, *49*, 9068−9093. (b) Anthony, J. *Angew. Chem., Int. Ed.* **2008**, *47*, 452−483.
(24) Motta, S. D.; Negri, F.; Fazzi, D.; Castiglioni, C.; Canesi, E. V. *J. Phys. Chem. Lett.* **2010**, *1*, 3334−3339.